Presynaptic serotonin 2A receptors modulate thalamocortical plasticity and associative learning

Alexander Barre[a,b,c,1], Coralie Berthoux[a,b,c,1], Dimitri De Bundel[a,b,c], Emmanuel Valjent[a,b,c], Joël Bockaert[a,b,c], Philippe Marin[a,b,c], and Carine Bécamel[a,b,c,2]

[a]Département de Neurosciences, Centre National de la Recherche Scientifique, UMR-5203, Institut de Génomique Fonctionnelle, F-34094 Montpellier, France; [b]Département de Neurosciences, Institut National de la Santé et de la Recherche Médicale, U1191, F-34094 Montpellier, France; and [c]Université de Montpellier, F-34094 Montpellier, France

Higher-level cognitive processes strongly depend on a complex interplay between mediodorsal thalamus nuclei and the prefrontal cortex (PFC). Alteration of thalamofrontal connectivity has been involved in cognitive deficits of schizophrenia. Prefrontal serotonin (5-HT)$_{2A}$ receptors play an essential role in cortical network activity, but the mechanism underlying their modulation of glutamatergic transmission and plasticity at thalamocortical synapses remains largely unexplored. Here, we show that 5-HT$_{2A}$ receptor activation enhances NMDA transmission and gates the induction of temporal-dependent plasticity mediated by NMDA receptors at thalamocortical synapses in acute PFC slices. Expressing 5-HT$_{2A}$ receptors in the mediodorsal thalamus (presynaptic site) of 5-HT$_{2A}$ receptor-deficient mice, but not in the PFC (postsynaptic site), using a viral gene-delivery approach, rescued the otherwise absent potentiation of NMDA transmission, induction of temporal plasticity, and deficit in associative memory. These results provide, to our knowledge, the first physiological evidence of a role of presynaptic 5-HT$_{2A}$ receptors located at thalamocortical synapses in the control of thalamofrontal connectivity and the associated cognitive functions.

serotonin | 5-HT$_{2A}$ receptors | thalamocortical synapse | presynaptic NMDA receptors | temporal-dependent plasticity

The prefrontal cortex (PFC) is a brain region critical for many high-level cognitive processes, such as executive functions, attention, and working and contextual memories (1). Pyramidal neurons located in layer V of the PFC integrate excitatory glutamatergic inputs originating from both cortical and subcortical areas. The latter include the mediodorsal thalamus (MD) nuclei, which project densely to the medial PFC (mPFC) and are part of the neuronal network underlying executive control and working memory (2–4). Disruption of this network has been involved in cognitive symptoms of psychiatric disorders, such as schizophrenia (3, 5). These symptoms severely compromise the quality of life of patients and remain poorly controlled by currently available antipsychotics (3, 6).

The PFC is densely innervated by serotonin (5-hydroxytryptamine, 5-HT) neurons originating from the dorsal and median raphe nuclei and numerous lines of evidence indicate a critical role of 5-HT in the control of emotional and cognitive functions depending on PFC activity (7, 8). The modulatory action of 5-HT reflects its complex pattern of effects on cortical network activity, depending on the 5-HT receptor subtypes involved, and on receptor localization in pyramidal neurons, GABAergic interneurons or nerve terminals of afferent neurons.

Among the 14 5-HT receptor subtypes, the 5-HT$_{2A}$ receptor is a Gq protein-coupled receptor (9, 10) particularly enriched in the mPFC, with a predominant expression in apical dendrites of layer V pyramidal neurons (11–14). Moreover, a low proportion of 5-HT$_{2A}$ receptors was detected presynaptically on thalamocortical fibers (12, 15–17).

Activation of 5-HT$_{2A}$ receptors exerts complex effects upon the activity of the PFC network (18). The most prominent one is an increase in pyramidal neuron excitability, which likely results from the inhibition of slow calcium-activated after hyperpolarization current

(19). 5-HT$_{2A}$ receptor stimulation also increases the frequency and amplitude of spontaneous excitatory postsynaptic currents (sEPSCs) in pyramidal neurons (19–22). The prevailing view is that postsynaptic 5-HT$_{2A}$ receptors expressed on pyramidal neurons located in layer V are key modulators of glutamatergic PFC network activity (14, 21–24). However, the role of presynaptic 5-HT$_{2A}$ receptors located on thalamic afferents in the modulation of glutamatergic transmission at thalamocortical synapses remains unexplored.

Here, we addressed this issue by combining electrophysiological recordings in acute PFC slices with viral infections to specifically rescue the expression of 5-HT$_{2A}$ receptors at the presynaptic site (MD) or postsynaptic site (PFC) in 5-HT$_{2A}$ receptor-deficient (5-HT$_{2A}^{-/-}$) mice (25). We focused our study on NMDA transmission in line with previous findings indicating that many symptoms of schizophrenia might arise from modifications in PFC connectivity involving glutamatergic transmission at NMDA receptors (26, 27). To our knowledge, we provide the first direct evidence that stimulation of presynaptic 5-HT$_{2A}$ receptors at thalamocortical synapses gates the induction of spike timing-dependent long-term depression (t-LTD) by facilitating the activation of presynaptic NMDA receptors at these synapses. In line with the role of t-LTD in associative learning (28), these studies were extended by behavioral experiments to explore the role of presynaptic 5-HT$_{2A}$ receptors at thalamocortical synapses in several paradigms of episodic-like memory.

Significance

Higher-level cognitive processes strongly depend on a complex interplay between the mediodorsal thalamus and the prefrontal cortex. Alteration of thalamofrontal connectivity has been involved in schizophrenia. Prefrontal serotonin (5-HT)$_{2A}$ receptors play an essential role in cortical network activity but the mechanism underlying their modulation of synaptic plasticity remains unexplored. Here, we demonstrate—to our knowledge for the first time—a physiological role of presynaptic 5-HT$_{2A}$ receptors in the NMDA-operated induction of temporal-dependent plasticity at thalamocortical synapses. We show that 5-HT$_{2A}^{-/-}$ mice exhibit alterations in plasticity and associative memory that are rescued by re-expressing receptors in the thalamus. These findings highlight a critical role of presynaptic 5-HT$_{2A}$ receptor dysfunction in cognitive symptoms observed in schizophrenia.

Results

Effect of 5-HT$_{2A}$ Receptor Activation on NMDA Transmission at Thalamocortical Synapses. We recorded isolated NMDA EPSCs elicited in layer V pyramidal neurons of rat mPFC slices by stimulating thalamic fibers, which represent the majority of axons projecting in layer I (2, 4). Because NMDA receptors have a dual need for glutamate and depolarization to be activated, NMDA EPSCs were recorded in two different conditions facilitating their detection: (*i*) at the resting potential in low magnesium artificial cerebrospinal fluid (ACSF) (29–31) and presence of 1,2,3,4-Tetrahydro-6-nitro-2,3-dioxo-benzo[f]quinoxaline-7-sulfonamide disodium salt hydrate (NBQX, 2 μM), an AMPA receptor antagonist; (*ii*) at a holding potential of +40 mV to relieve the voltage-dependent magnesium block at postsynaptic NMDA receptors (30).

In low-magnesium conditions, bath application of the 5-HT$_{2A}$ receptor agonist 2,5-dimethoxy-4-iodoamphetamine (DOI, 1 μM) produced a significant increase in the amplitude of NMDA EPSCs in juvenile (baseline: 26.95 ± 2.77 pA, DOI: 46.71 ± 6.70 pA; $P < 0.001$) (Fig. 1*A*) and adult rats and mice (Fig. S1), which was rapidly reversible after washout. This potentiation of NMDA currents was prevented by a pretreatment of slices with ketanserin (1 μM), a 5-HT$_{2A/2C}$ antagonist (baseline: 34.04 ± 6.43 pA, DOI: 26.48 ± 4.26 pA; $P > 0.05$) (Fig. 1*B*), and was not observed in slices from 5-HT$_{2A}$ receptor-deficient mice (5-HT$_{2A}$$^{-/-}$, baseline: 29.22 ± 1.92 pA, DOI: 28.16 ± 1.48 pA; $P > 0.05$) (Fig. 1*C*), consistent with a specific role of 5-HT$_{2A}$ receptors. In the presence of magnesium, NMDA EPSCs were not affected by DOI application (baseline: 24.33 ± 5.89 pA, DOI: 22.64 ± 5.93 pA; $P > 0.05$) (Fig. 1*D*) at a holding potential of +40 mV. The lack of effect of DOI in the experimental condition allowing the selective engagement of postsynaptic NMDA receptors (in ACSF containing magnesium) suggests that 5-HT$_{2A}$ receptor stimulation might affect the activity of presynaptic NMDA receptors located on thalamic fibers (31).

The 5-HT$_{2A}$ Receptors Modulate Neurotransmitter Release by Facilitating Presynaptic NMDA Receptors. To confirm the presynaptic origin of 5-HT$_{2A}$ receptor-mediated potentiation, we analyzed the paired pulse ratio (PPR) of NMDA EPSCs before and after DOI application. DOI treatment decreased the PPR (baseline: 1.07 ± 0.10, DOI: 0.68 ± 0.07; $P < 0.01$) (Fig. 1*E*). This finding suggests a presynaptic modification leading to an increase in neurotransmitter release probability (32), a process that might account for the observed potentiation of postsynaptic NMDA currents. Consistent with this hypothesis, bath application of DOI increased the frequency of AMPA-mediated miniature EPSCs (mEPSCs) in low-magnesium ACSF (baseline: 7.94 ± 0.86 Hz, DOI: 11.65 ± 0.95 Hz; $P < 0.001$) (Fig. S2*A*) when MK-801 was added into the recording pipette to block postsynaptic NMDA receptors (33). The DOI-elicited increase in mEPSC frequency was absent when recordings were performed with magnesium in the extracellular medium (Fig. S2*B*) and in slices pretreated with the competitive NMDA receptor antagonist D,L-2-Amino-5-phosphonopentanoic acid (D,L-AP5, 100 μM) (Fig. S2*C*). This result further supports the involvement of presynaptic NMDA receptors, as they also require simultaneous depolarization-induced removal of Mg^{2+} and glutamate binding to modulate glutamate release. Collectively, these observations show that 5-HT$_{2A}$ receptor activation enhances the frequency of glutamate release at excitatory synapses onto layer V mPFC neurons via a mechanism depending on presynaptic NMDA receptors.

Restoration of 5-HT$_{2A}$ Receptor Expression in the MD of 5-HT$_{2A}$$^{-/-}$ Mice Rescues Potentiation of NMDA Transmission at Thalamocortical Synapses. We thus hypothesized that the observed potentiation of NDMA transmission might result from a local modulation of presynaptic NMDA receptors by presynaptic 5-HT$_{2A}$ receptors (12, 15, 16). To demonstrate expression of 5-HT$_{2A}$ receptors at presynaptic sites in our cortical slices model, we first performed a fractionation procedure that permits enrichment in pre- and
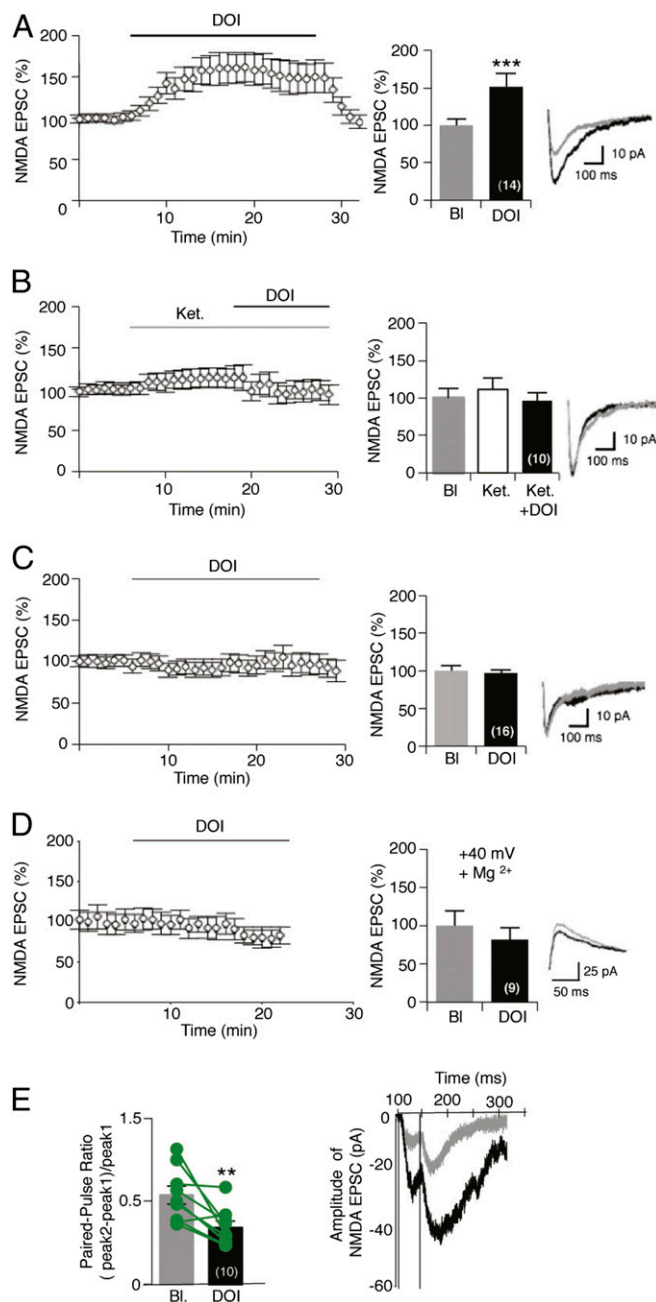

Fig. 1. 5-HT$_{2A}$ receptor activation potentiates NMDA EPSCs in PFC pyramidal neurons. (*A–C*) Normalized peak amplitude of isolated NMDA currents recorded in acute PFC slices at −60 mV in low magnesium ACSF are illustrated (*Left*). The histograms represent means ± SEM of NMDA EPSCs (in percent of baseline) measured during the last 2 min of baseline or treatments. In *A*, slices were perfused with DOI (1 μM) for 20 min ($n = 14$). ***$P < 0.001$ vs. baseline (Bl) (Student's *t* test). (*Right*) Representative traces of NMDA EPSCs. In *B*, Ketanserin (Ket, 1 μM) was perfused in the bath for 12 min before the application of DOI ($n = 10$, Student's *t* test). In *C*, NMDA currents were measured in acute PFC slices from 5-HT$_{2A}$$^{-/-}$ mice ($n = 16$, Student's *t* test). (*D*) Normalized amplitude of NMDA currents recorded at +40 mV in presence of magnesium ($n = 9$, Student's *t* test). The histogram represents means ± SEM of NMDA EPSCs (in percent of baseline) measured during the last 2 min of baseline or treatments. (*Right*) Representative traces of NMDA EPSCs at +40 mV. (*E*) Presynaptic origin of 5-HT$_{2A}$ receptor-mediated potentiation of NMDA EPSCs. Paired-pulse facilitation [(peak2 − peak1)/peak1] with 50 ms of interval, measured before (baseline) and after the DOI challenge (1 μM, 10 min, $n = 10$). **$P < 0.01$ vs. baseline, Student's *t* test. (*Right*) Representative traces of NMDA EPSCs. See also Figs. S1 and S2.

postsynaptic compartments from synaptosomal preparations. We detected a substantial amount of both $5\text{-}HT_{2A}$ receptors and NMDA receptors (GluN1 and GluN2B subunits) in the presynaptic compartment purified from cingulate, prelimbic and infralimbic areas of mPFC slices (Fig. S3). To further demonstrate the role of presynaptic $5\text{-}HT_{2A}$ receptors specifically located on thalamocortical fibers in the potentiation of NMDA trans-

mission, we selectively restored $5\text{-}HT_{2A}$ receptor expression in the mPFC (postsynaptic rescue) (Fig. 2B) or in MD nuclei (presynaptic rescue) (Fig. 2C) of $5\text{-}HT_{2A}^{-/-}$ mice (25). We used a Sindbis virus-based in vivo recombinant DNA-delivery technique (34) and a bicistronic construct coexpressing the $5\text{-}HT_{2A}$ receptor and GFP ($5\text{-}HT_{2A}$R-IRES-GFP) using an internal ribosomal entry site (IRES-GFP)] to detect infected neurons in both the mPFC and

Fig. 2. Expression of $5\text{-}HT_{2A}$ receptor in MD nuclei rescues DOI-induced potentiation of NMDA EPSCs in $5\text{-}HT_{2A}^{-/-}$ mice. (A and B) The *Left* panels show a sketch of the experimental protocol. Sindbis viruses expressing GFP constructs (A) or $5\text{-}HT_{2A}$-IRES-GFP (B) were injected in the PFC of WT (A) or $5\text{-}HT_{2A}^{-/-}$ (B) mice, respectively. Paired recordings were performed 24 h after viral particle injection in nearby infected (green) and noninfected (black) layer V pyramidal neurons. Representative traces of NMDA EPSCs are shown in black (noninfected neuron) and in green (infected neuron). The normalized amplitude of NMDA currents measured before (Baseline) and after DOI application (1 μM, 20 min) in infected (I) neurons was plotted against the normalized amplitude of NMDA EPSCs in noninfected (NI) neurons. The red dot indicates the mean of all values. The histograms show the quantification of NMDA EPSCs after DOI application (normalized to baseline) in simultaneously recorded infected (green) and noninfected (white) layer V neurons. n.s., not significant. (C) A sketch of the experimental protocol is shown in left. Sindbis viruses were injected at P14 in the MD nuclei (MDN) of $5\text{-}HT_{2A}^{-/-}$ mice. Representative traces of NMDA EPSCs are shown. The right histogram represents the percentage of recorded neurons showing a potentiation of NMDA EPSCs after the DOI challenge in 16 of 18, 4 of 16, 3 of 13, and 21 of 32 recorded cells in WT mice, $5\text{-}HT_{2A}^{-/-}$ mice (KO), postsynaptic rescued (Post R.) and presynaptic rescued (Pre R.) $5\text{-}HT_{2A}^{-/-}$ mice, respectively. The distribution of values measured in each condition is illustrated (*Right*). (D) Time course of normalized peak amplitude of isolated NMDA currents recorded in DOI-treated PFC slices from $5\text{-}HT_{2A}^{-/-}$ mice (KO, gray dots, n = 13), postsynaptic rescued $5\text{-}HT_{2A}^{-/-}$ mice (Post R., empty diamonds, n = 13) and presynaptic rescued $5\text{-}HT_{2A}^{-/-}$ mice (Pre R., full diamonds, only cells showing potentiation were plotted, n = 21). The histograms represent means ± SEM of NMDA EPSCs (in percent of baseline) measured during the last 2 min of baseline or DOI treatment. ***$P < 0.001$ vs. baseline (Bl), Student's t test. See also Figs. S3 and S4.

the thalamus (Fig. S4 *A* and *B*). In PFC-infected WT animals, recombinant receptors were mainly detected in pyramidal neurons of the mPFC, similar to endogenous 5-HT$_{2A}$ receptors (Fig. S4C). The strong overlap of recombinant and native receptors indicate a limited ectopic receptor expression following viral infection, even though some neurons that do not express 5-HT$_{2A}$ receptors in WT mice might also be infected. Paired-recording performed in acute slices from WT mice infected with GFP alone did not show any differences between infected and noninfected neurons, and evoked NMDA EPSCs were similarly enhanced upon 5-HT$_{2A}$ receptor activation in both infected and noninfected pyramidal neurons (Fig. 2A). This finding indicates that viral infection did not affect NMDA transmission and its potentiation by 5-HT$_{2A}$ receptors. The amplitude of NMDA EPSCs in cortical pyramidal neurons of postsynaptic rescued 5-HT$_{2A}$$^{-/-}$ mice was not different from that measured in nearby control noninfected neurons (receiving the same stimulation) following DOI application, suggesting that postsynaptic 5-HT$_{2A}$ receptors are not involved in the modulation of NMDA transmission

(Fig. 2B). In contrast, expression of 5-HT$_{2A}$ receptors in the MD nuclei of 5-HT$_{2A}$$^{-/-}$ mice substantially increased the proportion of neurons showing a potentiation of NMDA EPSCs upon DOI treatment (65% of recorded neurons in MD-infected 5-HT$_{2A}$$^{-/-}$ mice vs. 25% in noninfected 5-HT$_{2A}$$^{-/-}$ mice) (Fig. 2C). Moreover, the time course of DOI effect in neurons showing a potentiation in the presynaptic rescue condition (Fig. 2D) was similar to that observed for WT neurons (Fig. 1A). Taken together, these rescue experiments strongly support a role of presynaptic 5-HT$_{2A}$ receptors in the potentiation of NMDA transmission at thalamocortical synapses.

The 5-HT$_{2A}$ Receptor-Mediated Potentiation of NMDA Synaptic Transmission Depends on Presynaptic Phospholipase C and PKC Activities. To identify the mechanism underlying the potentiation of NMDA currents by 5-HT$_{2A}$ receptors, we used inhibitors of downstream effectors of 5-HT$_{2A}$ receptors. Pretreatment of slices with (S)-2,6-Diamino-*N*-[(1-(1-oxotridecyl)-2-piperidinyl)methyl]hexanamide dihydrochloride hydrate (NPC15437; 20 μM), a selective PKC inhibitor (35), or with
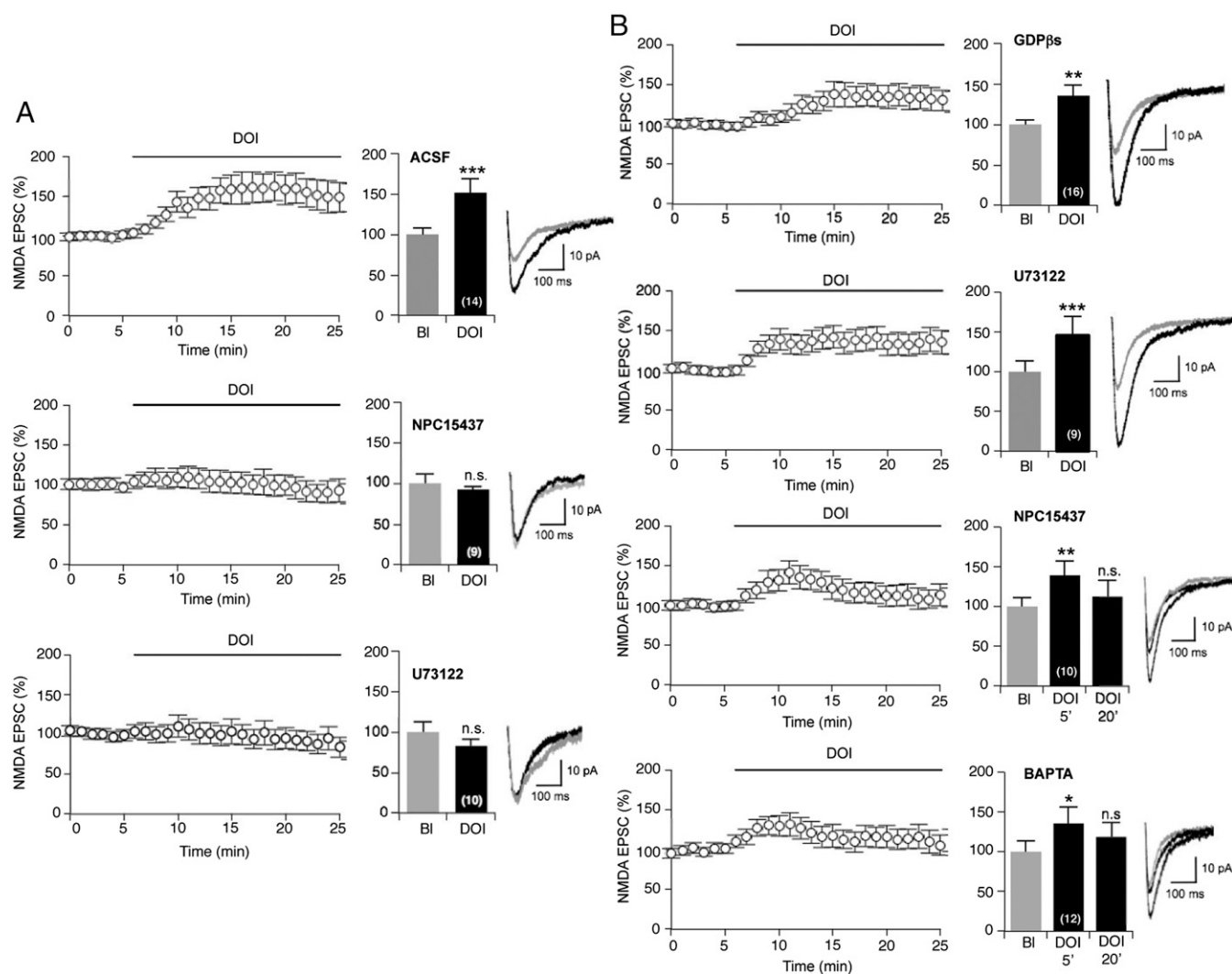

Fig. 3. Presynaptic PLC and PKC activities are necessary for DOI-elicited potentiation of NMDA currents. (*A*) Preincubation of slices for 10 min with the PKC inhibitor NPC15437 (20 μM, *n* = 9) or the PLC inhibitor U73122 (5 μM, *n* = 10) prevents potentiation of NMDA EPSCs induced by DOI. Note that the top graph is the same graph as that illustrated on Fig. 1A. (*B*) Loading recorded layer V neurons with the G protein inhibitor GDPβS (1 mM, *n* = 16) or with U73122 (5 μM, *n* = 9) has no effect on the potentiation of NMDA currents, whereas intracellular perfusion of the PKC inhibitor NPC15437 (20 μM, *n* = 10), or the calcium chelator BAPTA (20 μM, *n* = 12), inhibits the late phase of potentiation. Plots showing the time course of NMDA EPSCs in response to the treatments are shown (*Left*). The histograms show the normalized peak amplitude of NMDA EPSCs. (*Right*) Representative traces of NMDA EPSCs before (gray) and after (black) DOI application. *$P < 0.05$; **$P < 0.01$; ***$P < 0.001$ vs. baseline (Bl); n.s., not significant (Student's *t* test or one-way ANOVA).
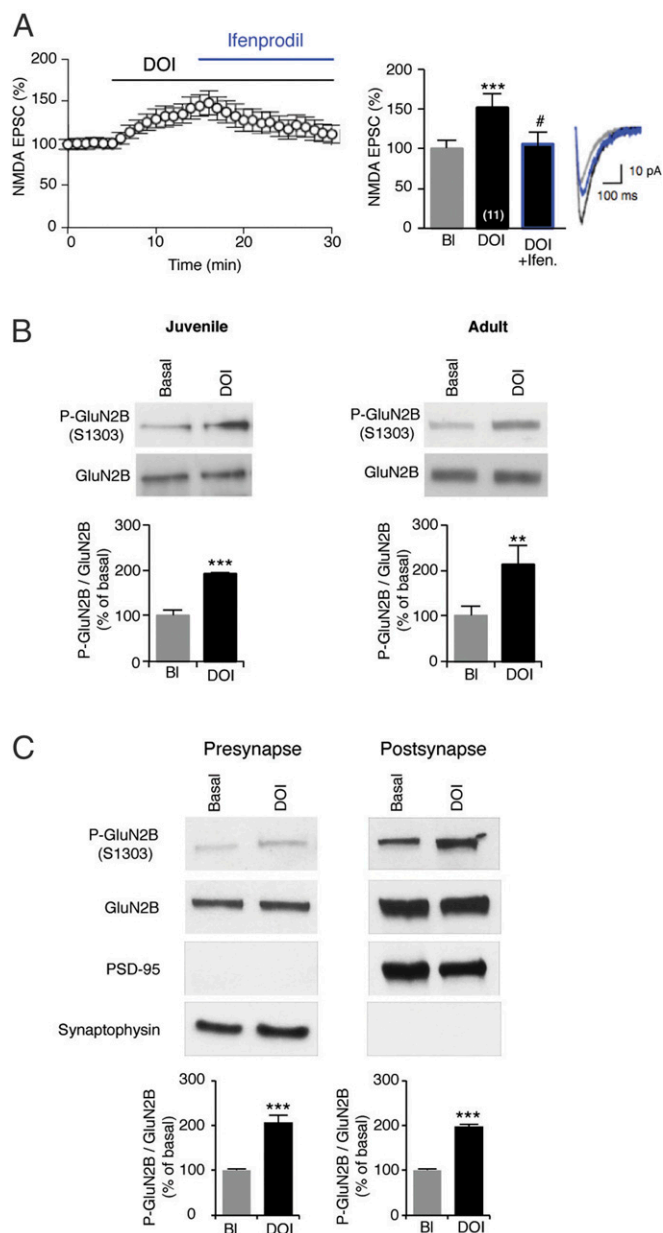
Fig. 4. DOI-elicited potentiation of NMDA EPSCs involves GluN2B-containing NMDA receptors. (*A*) After a period of baseline, DOI (1 μM) and ifenprodil (3 μM, n = 11), a specific antagonist of GluN2B-containing NMDA receptors, were successively perfused in the bath. (*Left*) The impact of drug application upon the normalized peak amplitude of NMDA EPSCs. The histogram shows the quantification of NMDA EPSCs, normalized to values obtained in baseline condition (Bl, gray bar), following DOI and ifenprodil applications. ***$P <$ 0.001 vs. baseline; #$P <$ 0.05 vs. DOI, one-way ANOVA followed by Newman–Keuls test. (*Right*) Representative traces of NMDA EPSCs before (gray) and after DOI (black) and ifenprodil (blue) applications. See also Fig. S5A. (*B*) Acute PFC slices from juvenile or adult rats were treated with either vehicle or DOI (1 μM) for 20 min. GluN2B phosphorylation at Ser^{1303} was assessed by sequential immunoblotting with a phospho-site specific antibody and an antibody recognizing GluN2B independently of its phosphorylation state. Representative Western blots are illustrated. Data, expressed in percent of baseline, represent ratios of phosphorylated to total GluN2B. They are the means ± SEM values obtained in three independent experiments. **$P <$ 0.01; ***$P <$ 0.001 vs. Bl. See also Fig. S5B. (*C*) Acute PFC slices from juvenile rats were treated with either vehicle or DOI (1 μM) for 20 min and used to prepare the synaptosomal fraction. Synaptosomes were treated with 1% TX-100 containing buffer, and equal quantities of proteins from soluble (presynapse) and insoluble fractions (postsynapse) were analyzed on Western blots probed with antibodies to the indicated proteins. As expected, PSD-95 was only detected in the postsynaptic

U73122 (5 μM), a phospholiphase C (PLC) inhibitor, abolished the increase in evoked NMDA EPSCs induced by DOI (Fig. 3*A*). To further explore the role of 5-HT$_{2A}$ receptor-operated PLC-PKC signaling in the presynaptic compartment, we next delivered inhibitors via the recording pipette. Addition of GDP-βS (1 mM) to block all G protein-dependent signaling pathways, or U73122 (5 μM) into the recording pipette, did not affect the potentiation of NMDA currents elicited by DOI (Fig. 3*B*). However, when NPC15437 (20 μM) or BAPTA (20 μM), a calcium chelator, was added into the pipette, DOI still produced a transient (10 min) potentiation of NMDA currents, which then returned to baseline after 15–20 min of DOI application (Fig. 3*B*). These results suggest that PKC and calcium-dependent signaling elicited by presynaptic 5-HT$_{2A}$ receptor activation trigger the earlier phase of the NMDA potentiation, whereas its maintenance might involve PKC and calcium-dependent signaling induced by postsynaptic 5-HT$_{2A}$ receptors.

The 5-HT$_{2A}$ Receptor Activation Induces GluN2B Phosphorylation at Ser^{1303}. NMDA receptors are heteromultimeric proteins composed of GluN1, GluN2A-D, and less commonly, GluN3A and GluN3B subunits, and NMDA receptor subunit composition varies between different brain regions and during development (36). Among these subunits, GluN2B has been involved in learning and associated plasticity in various brain structures, including the mPFC (30, 37). Therefore, we examined whether GluN2B-containing receptors are affected by DOI treatment using ifenprodil, a specific antagonist of GluN2B-containing receptors (38). Perfusion of slices with ifenprodil (3 μM) (30) did not significantly modify basal NMDA transmission in our recording conditions (Fig. S5A). When ifenprodil was perfused 10 min after the onset of DOI application, potentiated NMDA currents were inhibited (Fig. 4*A*), suggesting that 5-HT$_{2A}$ receptor activation selectively enhances EPSCs mediated by GluN2B-containing NMDA receptors.

Several lines of evidence support a role for PKC in potentiating NMDA receptor function (39, 40). PKC phosphorylates GluN2B subunit on serine residues (Ser^{1303} or Ser^{1323}) located in its carboxyl-terminal domain (41), and each of these phosphorylations induces a potentiation of NMDA currents (41, 42). To determine whether 5-HT$_{2A}$ receptor activation elicits GluN2B phosphorylation, acute PFC slices from juvenile and adult animals were exposed to DOI and Ser^{1303} phosphorylation state was analyzed in synaptosomal enriched fraction by Western blotting using a phospho-site specific antibody. Treating slices with DOI induced an increase in Ser^{1303} phosphorylation (Fig. 4*B*). As expected, the phosphorylation state of GluN2B was not modified by DOI in samples made from 5-HT$_{2A}^{-/-}$ mice (Fig. S5B). Furthermore, Ser^{1303} phosphorylation state was similarly enhanced by DOI application in both presynaptic and postsynaptic fractions obtained from synaptosomes (Fig. 4*C*), suggesting a functional coupling between 5-HT$_{2A}$ receptors with GluN2B-containing NMDA receptors.

Presynaptic 5-HT$_{2A}$ Receptor Activation Gates Presynaptic NMDA Receptor-Operated Induction of t-LTD. The t-LTD is a neural substrate of some forms of learning and memory that depends on the precise timing of a presynaptic input and a postsynaptic action potential (28). t-LTD occurs when a postsynaptic spike is followed by a presynaptic spike and reflects presynaptic changes in neurotransmitter release that specifically rely on activation of presynaptic NMDA receptors (43). To explore the impact of 5-HT$_{2A}$ receptor stimulation upon t-LTD induction at thalamocortical synapses, we used a protocol consisting of 75 pairings of an action potential at a layer V pyramidal neuron preceding a layer I-generated EPSP. This

fraction, whereas synaptophysin was exclusively found in the presynaptic fraction. Representative Western blots are illustrated. Data were expressed as in *B*. ***$P <$ 0.001 vs. Bl.

pairing protocol induced t-LTD at layer I/V synapses in the absence (Fig. S6 *A* and *E*) but not in the presence of magnesium in the extracellular medium (Fig. S6 *B* and *E*). Notably, in the presence of magnesium, this protocol induced t-LTD in slices only when DOI was perfused (for 2.5 min) during the pairing (Fig. S6 *B* and *E*). Moreover, t-LTD was induced even when postsynaptic NMDA receptors were blocked by the addition of MK-801 into the recording pipette (Fig. S6 *C* and *E*). In this condition, perfusion of D,L-AP5 (100 μM) in the recording chamber abolished 5-HT$_{2A}$ receptor-dependent t-LTD induction (Fig. S6 *C* and *F*). DOI application combined to a sole presynaptic stimulus produced no persistent change in synaptic strength (Fig. S6 *D* and *E*). This finding indicates that coincident presynaptic and postsynaptic activities are necessary to induce temporal-dependent plasticity at thalamocortical synapses, via a mechanism requiring modulation of NMDA receptors by 5-HT$_{2A}$ receptor at the presynapse.

To confirm the prominent role of presynaptic 5-HT$_{2A}$ receptors in the induction of t-LTD at thalamocortical synapses, we performed the same experiments in 5-HT$_{2A}$$^{-/-}$, PFC-infected 5-HT$_{2A}$$^{-/-}$, and MD-infected 5-HT$_{2A}$$^{-/-}$ mice, as well as in PFC-infected WT mice. As expected, the subthreshold pairing protocol induced t-LTD at layer I/V synapses in WT mice as well as in PFC-infected WT mice when DOI was perfused in the extracellular medium during the pairing (Fig. 5 *A* and *D*), but not in 5-HT$_{2A}$$^{-/-}$ mice (Fig. 5 *B* and *D*). t-LTD was rescued in MD-infected 5-HT$_{2A}$$^{-/-}$ mice (Fig. 5 *C* and *D*), but not in PFC-infected 5-HT$_{2A}$$^{-/-}$ mice (Fig. 5 *B* and *D*), further supporting the crucial role of presynaptic 5-HT$_{2A}$ receptors in the induction of t-LTD at layer I/V synapses.
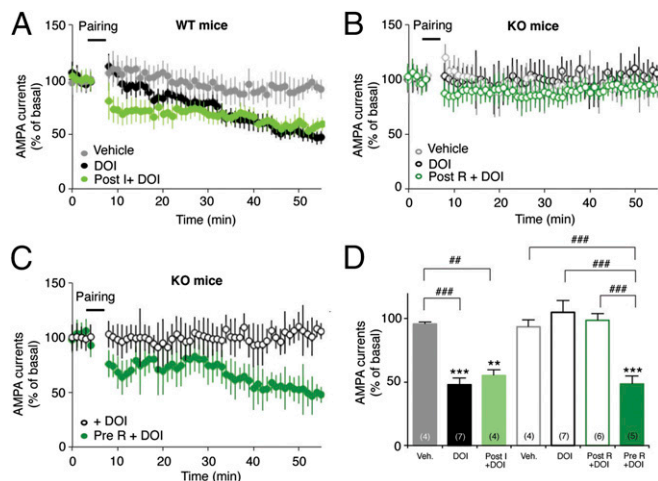

Fig. 5. Presynaptic 5-HT$_{2A}$ receptors are required for the induction of t-LTD at thalamocortical synapses. (*A*) A post-before-pre pairing protocol, consisting in five spikes at 10 Hz paired 15 times every 10 s with MK-801 (1 mM) delivered into the recording pipette induces t-LTD at thalamocortical synapses in acute PFC slices from WT mice only when DOI (1 μM) was applied in the bath (containing normal ACSF with 1 mM MgCl$_2$ and 2 mM CaCl$_2$) during the pairing protocol. The graph shows average AMPA currents recorded for 45 min after pairing performed in absence (n = 4, P > 0.05; gray dots) or presence of DOI in slices from WT mice (n = 7, P < 0.001; black dots) and of PFC-infected WT mice (postsynaptic infection, Post I., n = 4, P < 0.01; green dots). (*B*) t-LTD induction was absent in PFC slices from 5-HT$_{2A}$$^{-/-}$ mice in both the absence (n = 4, P > 0.05; opened gray dots) or presence of DOI (n = 7, P > 0.05; open black dots) as well as in PFC-infected 5-HT$_{2A}$$^{-/-}$ mice (Post R.) in the presence of DOI (n = 6, P > 0.05; open green dots). (*C*) t-LTD induction was restored in PFC slices from MD-infected 5-HT$_{2A}$$^{-/-}$ mice (Pre R.) when DOI was perfused during the pairing protocol (n = 5, P < 0.001; green dots). (*D*) Quantification of depression at 45–50 min after pairing. **P < 0.01, ***P < 0.001 vs. the corresponding baseline; ##P < 0.01, ###P < 0.001; one-way ANOVA followed by Newman–Keuls test. See also Fig. S6.

Presynaptic 5-HT$_{2A}$ Receptors on Thalamocortical Afferents Are Essential for Associative Learning. Several studies support a role for 5-HT$_{2A}$ receptors in episodic memory in humans (44, 45) and in rodent models (46). Recently, the mPFC and MD nuclei were found to cooperate within an integrated neural circuit to support associative learning, a key feature of episodic memory, and disruption of the thalamocortical pathway impaired learning of object-in-place associations (47). Furthermore, the temporal relationship of spike timing-dependent plasticity resembles typical features of associative learning (28). More specifically, t-LTD may be instrumental in the encoding of multimodal aspects of episodic-like memory such as associative memory (48, 49).

This finding prompted us to investigate the role of synaptic changes triggered by 5-HT$_{2A}$ receptor activation in three behavioral tasks addressing specific features of episodic-like memory: the novel-object recognition and novel-object location tasks (single item recognition), and the object-in-place task (distinguishes between multiple familiar items in their original or novel configuration). Memory retention was evaluated 1 h after the training session in all tasks. 5-HT$_{2A}$$^{-/-}$ mice were able to discriminate between novel and familiar objects [recognition index (RI): 0.26 ± 0.05 and 0.32 ± 0.05 for WT and 5-HT$_{2A}$$^{-/-}$ mice, respectively; P > 0.05] (Fig. 6*A*) and showed significant discrimination between novel and familiar object locations (RI: 0.47 ± 0.06 and 0.37 ± 0.05 for WT and 5-HT$_{2A}$$^{-/-}$ mice, respectively; P > 0.05) (Fig. 6*B*). However, 5-HT$_{2A}$$^{-/-}$ mice did not discriminate between familiar and novel object configurations in the object-in-place task (RI: 0.43 ± 0.04 and 0.09 ± 0.06 for WT and 5-HT$_{2A}$$^{-/-}$ mice, respectively; P < 0.001) (Fig. 6*C*). This finding indicates that 5-HT$_{2A}$ receptors are essential for learning object-in-place configurations. To determine whether presynaptic 5-HT$_{2A}$ receptors at thalamocortical synapses modulate this aspect of episodic-like memory, we specifically restored the expression of 5-HT$_{2A}$ receptors in the MD nuclei of 5-HT$_{2A}$$^{-/-}$ mice by bilateral injection of the 5-HT$_{2A}$-IRES-GFP viral construct. WT or 5-HT$_{2A}$$^{-/-}$ mice that were injected bilaterally with the GFP control virus into the MD nuclei did not differ from noninfected mice in the object-in-place task, indicating that surgery and viral infection did not affect associative learning. Presynaptic rescued 5-HT$_{2A}$$^{-/-}$ mice showed a similar performance to the WT animals (RI: 0.30 ± 0.05, 0.005 ± 0.06, and 0.32 ± 0.08 for WT mice infected with GFP, 5-HT$_{2A}$$^{-/-}$ mice infected with GFP, and 5-HT$_{2A}$$^{-/-}$ mice infected with 5-HT$_{2A}$ receptors viral constructs, respectively) (Fig. 6*D*). All presynaptic rescued mice used for behavioral analyses showed a clear bilateral infection of the MD, as assessed by GFP fluorescence (Fig. 6*D*). Collectively, these results demonstrate the crucial role of presynaptic 5-HT$_{2A}$ receptors located on thalamocortical afferents in associative memory.

Discussion

A large body of evidence indicates a critical role of 5-HT$_{2A}$ receptors in the modulation of glutamatergic transmission in the PFC. The most prominent effect elicited by the activation of these receptors is an increase of both spontaneous glutamate-mediated synaptic activity and pharmacologically induced NMDA currents (20, 50, 51). It has been hypothesized that they result from an increase in glutamate release from thalamocortical fibers elicited by either activation of presynaptic 5-HT$_{2A}$ receptors expressed on thalamocortical axons/terminals or a putative retrograde messenger produced by pyramidal neurons upon activation of postsynaptic receptors (21, 23). The current view rather supports an activation of the intrinsic cortical network via the excitation of a subpopulation of pyramidal neurons located in deep layers of the PFC (24). However, these studies investigated the influence of 5-HT$_{2A}$ receptors on global cortical glutamatergic transmission in the PFC and direct evidence of a modulation of synaptic transmission at thalamocortical synapses by 5-HT$_{2A}$ receptors was lacking. Here, we addressed this issue by measuring EPSCs evoked in layer V pyramidal neurons by the direct stimulation of
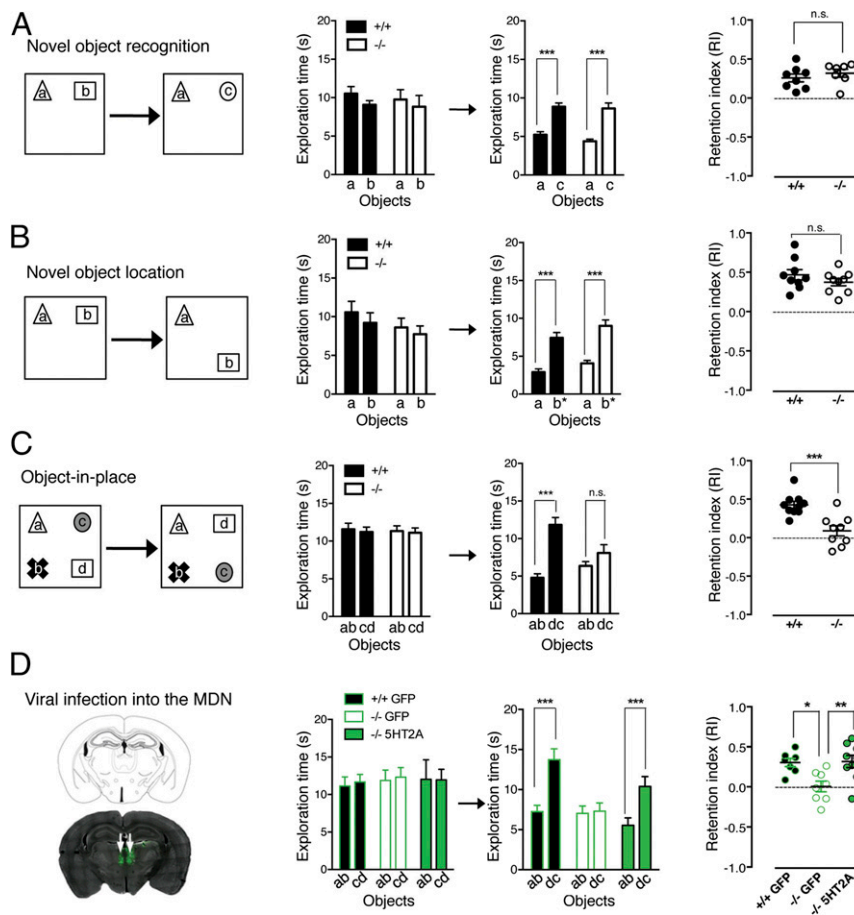
Fig. 6. Presynaptic 5-HT$_{2A}$ receptors at thalamocortical synapses are essential to associative learning. (*A–C*) Performance of WT (black bars) and 5-HT$_{2A}$$^{-/-}$ (white bars) mice in the novel-object recognition (*A*), novel-object location (*B*), and object-in-place (*C*) tasks performed using a 1-h intersession delay. Schemas of the protocols used for the different tasks are shown (*Left*). The plots on the right show the recognition memory for each task, expressed as the retention index. During the 5-min exploration phase, the mice within each group spent the same time exploring each of the two or four objects (*Left* histograms). "a," "b," "c," and "d" represent the different objects used during the task, as shown *Left*. After a 1-h delay, the absence of 5-HT$_{2A}$ receptors does not alter novel object recognition or object location performance (*A* and *B*) but affected the performance of mice in the object-in-place test (*C*). (*D*) Expression of 5-HT$_{2A}$ receptors in the thalamus MD nuclei (MDN) of 5-HT$_{2A}$$^{-/-}$ mice restores the WT phenotype in the object-in-place test. The image on the left illustrates the efficient re-expression of 5-HT$_{2A}$ receptors, as assessed by GFP detection, in the MD nuclei of 5-HT$_{2A}$$^{-/-}$ mice 24 h after the injection of viral particles. *$P < 0.05$; **$P < 0.01$; ***$P < 0.001$; n.s., not significant, Mann–Whitney test, $n = 7$–10 mice per group.

thalamocortical afferents in layer I. We found that the activation of 5-HT$_{2A}$ receptors expressed on thalamic neurons from MD nuclei (17) increases NMDA EPSCs, thus providing evidence that presynaptic 5-HT$_{2A}$ receptors enhance glutamatergic transmission in the PFC. Expression of endogenous 5-HT$_{2A}$ receptors could not be established by immunohistochemistry in thalamo-cortical afferents because of their sparse presynaptic expression. Nonetheless, the rescue of the potentiation of NMDA transmission in 5-HT$_{2A}$$^{-/-}$ mice by the specific expression (using a viral strategy) of 5-HT$_{2A}$ receptors in MD nuclei, but not by the restoration of their expression in the PFC, provided strong functional evidence of their role in the modulation of synaptic transmission at these synapses. Notably, the DOI-elicited potentiation was restored in 21 of 32 recorded neurons from MD-infected 5-HT$_{2A}$$^{-/-}$ mice, an observation likely reflecting the lack of infection of a fraction of MD neurons connected to layer V pyramidal neurons. However, this rescue strategy was more relevant than knocking down the expression of postsynaptic 5-HT$_{2A}$ receptors in the PFC of WT mice using a shRNA, as the initial events underlying the potentiation of glutamatergic transmission can arise from the excitation of a nearby noninfected pyramidal neuron, (i.e., a neuron still expressing 5-HT$_{2A}$ receptors) (24). Accordingly, 5-HT$_{2A}$–mediated potentiation of NMDA transmission could be detected even in neurons that do not express postsynaptic 5-HT$_{2A}$ receptors, precluding any clear

conclusion from such knockdown experiments. In contrast with the present findings, a previous report has shown that the lesion of the thalamus (including the MD nuclei that project to the median PFC) did not alter the excitatory effect of DOI on py-ramidal neuron firing and 5-HT release, even though the base-line firing of pyramidal neurons in thalamic lesioned rats was largely decreased compared with control rats, reflecting a marked loss of excitatory inputs (4). This study suggests a prominent role of postsynaptic 5-HT$_{2A}$ receptors in the control of the overall firing activity of cortical pyramidal neurons, consistent with their pre-dominant localization on apical dendrites of these neurons, whereas presynaptic receptors located on thalamocortical afferents specifi-cally influence glutamatergic transmission at thalamocortical synapses.

We obtained much electrophysiological evidence consistent with a presynaptic origin of the potentiation of glutamatergic transmission elicited by the stimulation of 5-HT$_{2A}$ receptors: the increase in evoked NMDA responses was associated with a modification in the PPR (52). Moreover, the frequency of AMPA mEPSCs was in-creased upon 5-HT$_{2A}$ receptor activation. We were also able to gain mechanistic insights into 5-HT$_{2A}$ receptor-dependent presynaptic enhancement: the increase in the evoked NMDA responses following 5-HT$_{2A}$ receptor activation was dependent on presynaptic PLC and PKC activities. PKC is known to phosphorylate several NMDA

receptor subunits, including GluN2B, to up-regulate NMDA receptor activity (39, 40). In line with these results, we found that stimulating 5-HT$_{2A}$ receptors with DOI induced the phosphorylation of GluN2B subunit at a PKC consensus site in PFC synaptosomes obtained from juvenile and adult rats. Moreover, blockade of DOI-elicited potentiation of NMDA currents by ifenprodil showed involvement of GluN2B-containing NMDA receptors. Although NMDA receptors were classically considered as postsynaptic receptors, increasing evidence indicates that they are also expressed presynaptically, and that up-regulation of presynaptic NMDA receptors enhances the probability of spontaneous and evoked neurotransmitter release at cortical, hippocampal, and cerebellar synapses (53). Moreover, the GluN2B subunit has been identified as one of the subunits of cortical presynaptic NMDA receptors (53), an observation confirmed in the present study. Collectively, these findings strongly support a mechanism whereby the activation of presynaptic 5-HT$_{2A}$ receptors expressed on thalamocortical afferents might locally induce, via PKC, the phosphorylation of presynaptic GluN2B-containing NMDA receptors. The resulting up-regulation of NMDA receptor function might in turn enhance the release of glutamate elicited by the stimulation of thalamocortical afferents, a process accounting for the increase in evoked NMDA EPSCs measured in slices treated with DOI.

In the present study, we also demonstrate that the activation of presynaptic 5-HT$_{2A}$ receptors facilitates the induction of t-LTD at thalamocortical synapses of the PFC. t-LTD induction was abolished in 5-HT$_{2A}$$^{-/-}$ mice but not in 5-HT$_{2A}$$^{-/-}$ mice in which 5-HT$_{2A}$ receptor expression was specifically rescued in MD nuclei using a viral strategy. This provides direct evidence of a regulatory role of presynaptic 5-HT$_{2A}$ receptors in spike timing-dependent plasticity. These observations are also consistent with a modulation of presynaptic NMDA receptors upon activation of 5-HT$_{2A}$ receptors, inasmuch as t-LTD induction has been found to specifically require presynaptic, but not postsynaptic, NMDA receptors (43). Several studies have suggested that the temporal relationship of spike timing-dependent plasticity resembles typical features of associative learning (28, 54). Consistent with these observations and the critical role of presynaptic 5-HT$_{2A}$ receptors in the induction of t-LTD, we found that 5-HT$_{2A}$$^{-/-}$ mice do not learn object-in-place associations, but show similar performance as WT mice in single-item recognition or location recognition tasks. These results also corroborate a recent report, which showed that the perfusion of MDL 11939, a 5-HT$_{2A}$ antagonist, into the PFC only alters object-in-place memory retrieval, but not single-item recognition (46). Such a phenotype was also induced by bilateral lesions not only in the PFC, but also in the MD nuclei, suggesting a complex interplay between both brain regions. Further supporting the critical role of connections between the MD nuclei and PFC in recognition memory when the discriminations involve associative information, contralateral lesions in MD nuclei and the PFC, but not ipsilateral lesions, similarly abolish novelty discrimination in the object-in-place task (47). In addition, 5-HT$_{2A}$$^{-/-}$ mice, in which 5-HT$_{2A}$ receptor expression was specifically restored in MD nuclei using a viral strategy, exhibited a similar performance as WT animals in the object-in-place task. Therefore, the present study provides strong experimental evidence that presynaptic 5-HT$_{2A}$ receptors at thalamocortical synapses play an essential role in associative learning and identifies, to our knowledge for the first time, a physiological function for presynaptic 5-HT$_{2A}$ receptors.

5-HT$_{2A}$ receptors in the PFC have long been known to have a critical influence in the pathogenesis of schizophrenia. They represent the primary target of second-generation antipsychotics, such as clozapine and its derivatives, and postsynaptic receptors located in PFC pyramidal neurons mediate the psychotropic effects of hallucinogens that are often used to probe positive symptoms (17, 55). PFC dysfunction has also been involved in cognitive symptoms and a recent study suggests that the disruption of thalamocortical connectivity might contribute to the deficits in episodic memory observed in patients with schizophrenia (3). Our study, which shows an alteration of associative memory in 5-HT$_{2A}$$^{-/-}$ mice that can be rescued by the re-expression of receptors in the MD, suggests that the dysfunction of presynaptic 5-HT$_{2A}$ receptors located on thalamocortical afferents might participate in cognitive symptoms observed in schizophrenia in addition to psychotic-like symptoms exerted by the activation of postsynaptic receptors. Accordingly, presynaptic 5-HT$_{2A}$ receptor blockade by second-generation antipsychotics, such as clozapine, might have deleterious effects upon some cognitive functions. These deleterious effects might minimize their procognitive action mediated by other targets (e.g., 5-HT$_6$ receptors) (56) and account for their low efficiency against the currently untreated and strongly debilitating cognitive symptoms of schizophrenia.

Materials and Methods

Animals. PFC slices were made from Sprague-Dawley rats or from C57 BL/6 WT mice or 5-HT$_{2A}$$^{-/-}$ mice. 5-HT$_{2A}$$^{-/-}$ mice, generated by the laboratory of Jay Gingrich (Mount Sinai School of Medicine, New York) (25), were kindly provided by Laurence Lanfumey (Centre de Psychiatrie et Neurosciences, Paris). Procedures were performed in strict compliance with the animal use and care guidelines of Montpellier University (authorization A34-518).

Drugs. DOI, ketanserin, MK801, picrotoxin, 1-[6-[((17β)-3-Methoxyestra-1,3,5[10]-trien-17-yl)amino]hexyl]-1H-pyrrole-2,5-dione (U73122), D,L-AP5, NPC15437, NBQX, and 2-chloroadenosine were obtained from Sigma-Aldrich and tetrodotoxin from Tocris.

Slice Preparation and Electrophysiological Recordings. Animals (14- to 18-d-old for juvenile or 50–60 d for adult) were anesthetized with isoflurane. Brains were removed and rapidly transferred into ice-cold dissection buffer [25 mM NaHCO$_3$, 1.25 mM NaH$_2$PO$_4$, 2.5 mM KCl, 0.5 mM CaCl$_2$, 7 mM MgCl$_2$, 25 mM glucose, 110 mM choline chloride, 11.6 mM ascorbic acid, 3.1 mM pyruvic acid maintained in 5% (vol/vol) CO$_2$/95% (vol/vol) O$_2$]. Coronal brain slices (300 μm) were cut in dissection buffer using a Vibratome (Campden Instruments) and transferred to ACSF (118 mM NaCl, 2.5 mM KCl, 26.2 mM NaHCO$_3$, 1 mM NaH$_2$PO$_4$, 11 mM glucose, 1 mM MgCl$_2$, 2 mM CaCl$_2$ maintained in 5% CO$_2$/95% O$_2$ at 22 °C–25 °C). The recording chamber was perfused with ACSF supplemented with 0.1 mM picrotoxin and 2 μM 2-chloroadenosine at 22 °C–25 °C. MgCl$_2$ was excluded from the ACSF in experiments performed in low-magnesium condition (31).

Patch recording pipettes (3–5 MΩ) were filled with intracellular solution (115 mM cesium gluconate, 20 mM CsCl, 10 mM Hepes, 2.5 mM MgCl$_2$, 4 mM Na$_2$ATP, 0.4 mM NaGTP, 10 mM sodium phosphocreatine, 0.6 mM EGTA, pH 7.3). Whole-cell recordings were obtained from infected or uninfected layer V pyramidal neurons (300–400 μm from pial surface) of the prelimbic or anterior cingulate subdivisions PFC using a Multiclamp 700B amplifier (Axon Instruments) under an Axioscope2 microscope (Zeiss) equipped with infrared differential interference contrast optics. Data were filtered at 2 kHz and sampled at 10 kHz using Digidata 1440A (Molecular Devices) under the control of pClamp 10 (Axon Instruments). There were no significant differences in input or series resistance among groups (infected, noninfected). Bipolar tungsten stimulating electrodes (from FHC) were placed in layer I (0–100 μm from pial surface). Stimulus intensity was increased until a synaptic response of amplitude > ~10 pA was recorded. For paired recordings, infected and nearby (~50 μm) noninfected neurons were whole-cell accessed and a synaptic response to stimulus was simultaneously recorded from both cells. In all experiments, EPSCs were evoked at a frequency of 0.33 Hz.

Drugs were administered in the perfusion medium unless otherwise indicated. Antagonists and pharmacological inhibitors were applied for 10 min before and during the DOI challenge. When drugs were loaded into the recording pipette, DOI was perfused in the recording chamber 15 min after the beginning of the patch.

mEPSCs were recorded in presence of TTX (1 μM). AMPA mEPSCs were recorded in absence or presence of magnesium (4 mM) and MK-801 (1 mM, delivered into the recording pipette) to block postsynaptic NMDA currents.

NMDA paired-pulse facilitation was performed in the same conditions as for NMDA EPSC recording, as previously described (32). Briefly, two NMDA EPSCs (EPSC1 and EPSC2) were evoked at 20 Hz, 10 times at 10-s intervals before and after 10 min of DOI perfusion. The PPR was calculated as (EPSC2-EPSC1)/EPSC1, where EPSC1 and EPSC2 represent the mean amplitudes of the first and second EPSCs, respectively. Traces from 10 pairs of EPSCs were averaged to obtain the means.

Induction of t-LTD. t-LTD was induced by post-before-pre firing at 20 Hz in rats (57) and 10 Hz in mice. Spike trains consisting of five spikes at 20 Hz or 10 Hz were paired 15 times every 10 s, thus producing a total of 75 spike pairings. Responses were monitored for 50 min after the induction of t-LTD. The quantification was made on the last 5 min of recording. Recordings were made at 29 °C. Internal solution contained 125 mM potassium gluconate, 10 mM KCl, 10 mM Hepes, 1.8 mM $MgCl_2$, 4 mM Na_2ATP, 0.3 mM NaGTP, 14 mM sodium phosphocreatine, 0.2 mM EGTA, pH 7.2. Physiological ACSF containing 1 mM $MgCl_2$ and 2 mM $CaCl_2$ was maintained in 5% CO_2/95% O_2 at 22 °C–25 °C. Data were analyzed using the GraphPad Prism software (v6.0) and statistical significance was determined by one-way ANOVA followed by Newman–Keuls test.

Viral Particle Production and Delivery. Human 5-HT$_{2A}$ receptor cDNA was subcloned in pIRES2-EGFP plasmid (Clontech) to allow coexpression with IRES-GFP. Viral infections in rescue experiments were performed using a modified Sindbis virus, which is neurotropic and does not infect glial cells (34). Viral particles were prepared as previously described (58). Briefly, the cDNA encoding 5-HT$_{2A}$ receptor was amplified by PCR and subcloned in pSinRep5 plasmid using Mlu1 restriction sites. This DNA construct was subsequently used to generate RNA transcripts (recombinant RNA) in vitro. Production of pseudovirions was then performed by transfecting BHK cells with the recombinant RNA and a helper RNA that provides the Sindbis structural proteins. Particles released by transfected BHK cells contain only the recombinant RNA. Mice were anesthetized with a ketamine/xylazine mixture (ketamine: 0.56-mg/g body weight; xylazine: 0.03-mg/g body weight). The skin overlying the skull was cut and gently pushed to the side. The anterior fontanel (Bregma) was identified and a region 1.95-mm anterior, 0.15-mm lateral [for the PFC from postnatal day (P)15 to P20], 1.1-mm posterior, 0.3-mm lateral (for the MD nuclei from P15 to P20), or 1.28-mm posterior, 0.5-mm lateral (for the MD nuclei at P60) was gently pierced with a dental drill. Glass pipettes (tip diameter ∼10 μm) were used to inject recombinant Sindbis viruses into the brain. After injection, the skin was repositioned and maintained with cyanoacrylate glue. During procedures, animals were kept on a heating pad and were brought back into their home cages after regaining movement. Infected mice were killed for slice preparation 24 h after infection.

Preparation of Pre- and Postsynapse-Enriched Fractions and Western Blotting. Acute PFC slices were exposed to vehicle or DOI (1 μM) for 20 min in ACSF. Synapse-enriched preparation was performed as described previously (59). All buffers contained 1 mM sodium orthovanadate, 50 mM sodium fluoride, 5 mM sodium pyrophosphate, and a mixture of protease inhibitors (Roche) to prevent degradation and dephosphorylation of proteins. Briefly, slices were homogenized in a buffer containing 0.32 M sucrose, 10 mM Hepes pH 7.4. Homogenates were cleared two times at 1,000 × g for 10 min to remove nuclei and large debris. The resulting supernatants were concentrated at 12,000 × g for 20 min to obtain a crude membrane fraction, which was rinsed twice (4 mM Hepes pH 7.4, 1 mM EDTA, 20 min at 12,000 × g). Samples were then resuspended in a buffer containing 20 mM Hepes pH 7.2, 100 mM NaCl and 0.5% Triton X-100 for 15 min and centrifuged at 12,000 × g for 20 min to pellet the synaptosomal membrane fraction. Separation of pre- and postsynaptic proteins was performed as previously described (60). Pellets were resuspended in 20 mM Tris, pH 6.0 and 1% TX-100 for 30 min at 4 °C and the insoluble material was centrifuged (40,000 × g, 30 min). Pellets were resuspended in 20 mM Tris, pH 8.0 and 1% TX-100 for 30 min at 4 °C to solubilize membrane proteins and samples were centrifuged (40,000 × g, 30 min) to separate presynaptic (supernatant) and postsynaptic (pellet) components. Protein concentration in each fraction was determined by the bicinchoninic acid method. Proteins were resolved on 10% gels and transferred electrophoretically onto nitrocellulose membranes (Hybond-C; GE Healthcare). Membranes were incubated in blocking buffer (Tris·HCl, 50 mM, pH 7.5; NaCl, 200 mM; Tween-20, 0.1% and skimmed dried milk, 5%) for 1 h at room temperature and overnight with primary antibodies in blocking buffer: rabbit anti-Phospho-S^{1303} GluN2B 1:500 (Millipore), mouse anti-GluN2B 1:500 (BD Biosciences), mouse anti-GluN1 1:500 (BD Biosciences), rabbit anti-5-HT$_{2A}$ receptor 1:250 (Immunostar), mouse anti-Synaptophysin 1:1,000 (Millipore), mouse anti-Munc18 1:5,000 (BD Biosciences), mouse anti–PSD-95 1:300 (NeuroMab). Membranes were then washed and incubated with horseradish peroxidase-conjugated anti-rabbit or anti-mouse antibodies (1:4,000 in blocking buffer; GE Healthcare) for 1 h at room temperature. Immunoreactivity was detected with an enhanced chemiluminescence method (ECL detection reagent; GE Healthcare).

Behavioral Analysis. Mice were extensively handled and habituated to the test before behavioral analysis. Testing was carried out in a Plexiglas box (35-cm width, 20-cm length, 20-cm height) placed in a dimly lit room with clearly visible contextual cues (black on white patterns) on the surrounding walls. Mice were habituated to the arena on days 1 and 2, for 10 min per day. On days 3, 4, and 5, mice performed the novel-object recognition task, object-location task, and object-in-place task, respectively. For the viral rescue experiments, mice were habituated to the arena on days 1 and 2, underwent viral injections on day 3, had an additional habituation to the arena on day 4, and performed the object-in-place task on day 5. For each of the tasks, the mice had a 5-min training session, a 1-h retention interval during which they were transferred back to the home cage, and a 5-min test session. The objects were plastic toys (∼3-cm width, 3-cm length, 5-cm height) and were cleaned with 10% ethanol between sessions. The experiments were video-recorded and object exploration times (nose in contact with the object or sniffing the object at <1 cm) were measured by a blinded observer. Data were analyzed using the GraphPad Prism software (v6.0) and statistical significance was determined by Mann–Whitney test. Animals were tested in three different tasks: novel-object recognition tasks, object-location task, and object-in-place task.
Novel-object recognition task. During the training phase, animals were allowed to explore two different objects for 5 min and placed in their home cage for 1 h, during which time the arena and objects were cleaned. Animals were then placed back into the arena in presence of an identical copy of one of the familiar objects and a novel object and allowed to explore the objects freely for 5 min. At the end of this recognition phase, animals were removed and returned to their home cage.
Object-location task. During the training phase, animals were allowed to explore two different objects for 5 min and placed in their home cage for 1 h. After this delay, the animals were placed back into the arena containing the objects present in the training sample phase. One of them was placed in the location previously occupied during the training phase, while the other one was placed in a new location within the arena. Object exploration was recorded for 5 min and animals were removed and returned to their home cage.
Object-in-place task. During the training session, animals were allowed to explore for 5 min four different objects placed in the four corners of the arena. The animals were removed from the arena for the delay period (1 h) and placed back in the arena that contains the same objects and where the positions of two objects were exchanged. Object exploration was recorded for 5 min.

Retention index [(exploration of novel object − exploration of familiar object)/total object exploration] was calculated for each test and analyzed by Mann–Whitney test.

1. Stuss DT, Knight RT, eds (2013) *Principles of Frontal Lobe Function* (Oxford Univ Press New York), 2nd Ed.
2. Berendse HW, Groenewegen HJ (1991) Restricted cortical termination fields of the midline and intralaminar thalamic nuclei in the rat. *Neuroscience* 42(1): 73–102.
3. Parnaudeau S, et al. (2013) Inhibition of mediodorsal thalamus disrupts thalamofrontal connectivity and cognition. *Neuron* 77(6):1151–1162.
4. Puig MV, Celada P, Díaz-Mataix L, Artigas F (2003) In vivo modulation of the activity of pyramidal neurons in the rat medial prefrontal cortex by 5-HT2A receptors: Relationship to thalamocortical afferents. *Cereb Cortex* 13(8):870–882.

5. Celada P, et al. (2013) Disruption of thalamocortical activity in schizophrenia models: Relevance to antipsychotic drug action. *Int J Neuropsychopharmacol* 16(10):2145–2163.
6. Antonova E, Sharma T, Morris R, Kumari V (2004) The relationship between brain structure and neurocognition in schizophrenia: A selective review. *Schizophr Res* 70(2-3):117–145.
7. Williams GV, Rao SG, Goldman-Rakic PS (2002) The physiological role of 5-HT2A receptors in working memory. *J Neurosci* 22(7):2843–2854.
8. Yan Z (2002) Regulation of GABAergic inhibition by serotonin signaling in prefrontal cortex: Molecular mechanisms and functional implications. *Mol Neurobiol* 26(2-3):203–216.

9. Roth BL, Berry SA, Kroeze WK, Willins DL, Kristiansen K (1998) Serotonin 5-HT2A receptors: Molecular biology and mechanisms of regulation. *Crit Rev Neurobiol* 12(4):319–338.

10. Marin P, Becamel C, Dumuis A, Bockaert J (2012) 5-HT receptor-associated protein networks: New targets for drug discovery in psychiatric disorders? *Curr Drug Targets* 13(1):28–52.

11. Willins DL, Deutch AY, Roth BL (1997) Serotonin 5-HT2A receptors are expressed on pyramidal cells and interneurons in the rat cortex. *Synapse* 27(1):79–82.

12. Jakab RL, Goldman-Rakic PS (1998) 5-Hydroxytryptamine2A serotonin receptors in the primate cerebral cortex: Possible site of action of hallucinogenic and antipsychotic drugs in pyramidal cell apical dendrites. *Proc Natl Acad Sci USA* 95(2):735–740.

13. Jakab RL, Goldman-Rakic PS (2000) Segregation of serotonin 5-HT2A and 5-HT3 receptors in inhibitory circuits of the primate cerebral cortex. *J Comp Neurol* 417(3):337–348.

14. Martín-Ruiz R, et al. (2001) Control of serotonergic function in medial prefrontal cortex by serotonin-2A receptors through a glutamate-dependent mechanism. *J Neurosci* 21(24):9856–9866.

15. Cornea-Hébert V, Riad M, Wu C, Singh SK, Descarries L (1999) Cellular and subcellular distribution of the serotonin 5-HT2A receptor in the central nervous system of adult rat. *J Comp Neurol* 409(2):187–209.

16. Miner LA, Backstrom JR, Sanders-Bush E, Sesack SR (2003) Ultrastructural localization of serotonin2A receptors in the middle layers of the rat prelimbic prefrontal cortex. *Neuroscience* 116(1):107–117.

17. González-Maeso J, et al. (2007) Hallucinogens recruit specific cortical 5-HT(2A) receptor-mediated signaling pathways to affect behavior. *Neuron* 53(3):439–452.

18. Celada P, Puig MV, Artigas F (2013) Serotonin modulation of cortical neurons and networks. *Front Integr Nuerosci* 7:25.

19. Araneda R, Andrade R (1991) 5-Hydroxytryptamine2 and 5-hydroxytryptamine 1A receptors mediate opposing responses on membrane excitability in rat association cortex. *Neuroscience* 40(2):399–412.

20. Aghajanian GK, Marek GJ (1997) Serotonin induces excitatory postsynaptic potentials in apical dendrites of neocortical pyramidal cells. *Neuropharmacology* 36(4-5):589–599.

21. Zhou FM, Hablitz JJ (1999) Activation of serotonin receptors modulates synaptic transmission in rat cerebral cortex. *J Neurophysiol* 82(6):2989–2999.

22. Lambe EK, Goldman-Rakic PS, Aghajanian GK (2000) Serotonin induces EPSCs preferentially in layer V pyramidal neurons of the frontal cortex in the rat. *Cereb Cortex* 10(10):974–980.

23. Marek GJ, Wright RA, Gewirtz JC, Schoepp DD (2001) A major role for thalamocortical afferents in serotonergic hallucinogen receptor function in the rat neocortex. *Neuroscience* 105(2):379–392.

24. Béïque JC, Imad M, Mladenovic L, Gingrich JA, Andrade R (2007) Mechanism of the 5-hydroxytryptamine 2A receptor-mediated facilitation of synaptic activity in prefrontal cortex. *Proc Natl Acad Sci USA* 104(23):9870–9875.

25. Weisstaub NV, et al. (2006) Cortical 5-HT2A receptor signaling modulates anxiety-like behaviors in mice. *Science* 313(5786):536–540.

26. Krystal JH, et al. (2000) Dissociation of ketamine effects on rule acquisition and rule implementation: Possible relevance to NMDA receptor contributions to executive cognitive functions. *Biol Psychiatry* 47(2):137–143.

27. Gilmour G, et al. (2012) NMDA receptors, cognition and schizophrenia—Testing the validity of the NMDA receptor hypofunction hypothesis. *Neuropharmacology* 62(3):1401–1412.

28. Letzkus JJ, Kampa BM, Stuart GJ (2007) Does spike timing-dependent synaptic plasticity underlie memory formation? *Clin Exp Pharmacol Physiol* 34(10):1070–1076.

29. Mayer ML, Westbrook GL, Guthrie PB (1984) Voltage-dependent block by Mg2+ of NMDA responses in spinal cord neurones. *Nature* 309(5965):261–263.

30. Barria A, Malinow R (2005) NMDA receptor subunit composition controls synaptic plasticity by regulating binding to CaMKII. *Neuron* 48(2):289–301.

31. Larsen RS, et al. (2011) NR3A-containing NMDARs promote neurotransmitter release and spike timing-dependent plasticity. *Nat Neurosci* 14(3):338–344.

32. Zinebi F, Russell RT, McKernan M, Shinnick-Gallagher P (2001) Comparison of paired-pulse facilitation of AMPA and NMDA synaptic currents in the lateral amygdala. *Synapse* 42(2):115–127.

33. Brasier DJ, Feldman DE (2008) Synapse-specific expression of functional presynaptic NMDA receptors in rat somatosensory cortex. *J Neurosci* 28(9):2199–2211.

34. Malinow R, et al. (2010) Introduction of green fluorescent protein (GFP) into hippocampal neurons through viral infection. *Cold Spring Harb Protoc* 2010(4):pdb.prot5406.

35. Sullivan JP, Connor JR, Shearer BG, Burch RM (1992) 2,6-Diamino-N-([1-(1-oxotridecyl)-2-piperidinyl] methyl)hexanamide (NPC 15437): A novel inhibitor of protein kinase C interacting at the regulatory domain. *Mol Pharmacol* 41(1):38–44.

36. Cull-Candy S, Brickley S, Farrant M (2001) NMDA receptor subunits: Diversity, development and disease. *Curr Opin Neurobiol* 11(3):327–335.

37. Tang YP, et al. (1999) Genetic enhancement of learning and memory in mice. *Nature* 401(6748):63–69.

38. Williams K (1993) Ifenprodil discriminates subtypes of the N-methyl-D-aspartate receptor: Selectivity and mechanisms at recombinant heteromeric receptors. *Mol Pharmacol* 44(4):851–859.

39. Lu WY, et al. (1999) G-protein-coupled receptors act via protein kinase C and Src to regulate NMDA receptors. *Nat Neurosci* 2(4):331–338.

40. Lin Y, Jover-Mengual T, Wong J, Bennett MV, Zukin RS (2006) PSD-95 and PKC converge in regulating NMDA receptor trafficking and gating. *Proc Natl Acad Sci USA* 103(52):19902–19907.

41. Liao GY, Wagner DA, Hsu MH, Leonard JP (2001) Evidence for direct protein kinase-C mediated modulation of N-methyl-D-aspartate receptor current. *Mol Pharmacol* 59(5):960–964.

42. Jones ML, Leonard JP (2005) PKC site mutations reveal differential modulation by insulin of NMDA receptors containing NR2A or NR2B subunits. *J Neurochem* 92(6):1431–1438.

43. Rodríguez-Moreno A, Paulsen O (2008) Spike timing-dependent long-term depression requires presynaptic NMDA receptors. *Nat Neurosci* 11(7):744–745.

44. de Quervain DJ, et al. (2003) A functional genetic variation of the 5-HT2a receptor affects human memory. *Nat Neurosci* 6(11):1141–1142.

45. Wagner M, Schuhmacher A, Schwab S, Zobel A, Maier W (2008) The His452Tyr variant of the gene encoding the 5-HT2A receptor is specifically associated with consolidation of episodic memory in humans. *Int J Neuropsychopharmacol* 11(8):1163–1167.

46. Bekinschtein P, Renner MC, Gonzalez MC, Weisstaub N (2013) Role of medial prefrontal cortex serotonin 2A receptors in the control of retrieval of recognition memory in rats. *J Neurosci* 33(40):15716–15725.

47. Cross L, Brown MW, Aggleton JP, Warburton EC (2012) The medial dorsal thalamic nucleus and the medial prefrontal cortex of the rat function together to support associative recognition and recency but not item recognition. *Learn Mem* 20(1):41–50.

48. Manahan-Vaughan D, Braunewell KH (1999) Novelty acquisition is associated with induction of hippocampal long-term depression. *Proc Natl Acad Sci USA* 96(15):8739–8744.

49. Braunewell KH, Manahan-Vaughan D (2001) Long-term depression: A cellular basis for learning? *Rev Neurosci* 12(2):121–140.

50. Arvanov VL, Liang X, Magro P, Roberts R, Wang RY (1999) A pre- and postsynaptic modulatory action of 5-HT and the 5-HT2A, 2C receptor agonist DOB on NMDA-evoked responses in the rat medial prefrontal cortex. *Eur J Neurosci* 11(8):2917–2934.

51. Lambe EK, Aghajanian GK (2006) Hallucinogen-induced UP states in the brain slice of rat prefrontal cortex: Role of glutamate spillover and NR2B-NMDA receptors. *Neuropsychopharmacology* 31(8):1682–1689.

52. Manabe T, Wyllie DJ, Perkel DJ, Nicoll RA (1993) Modulation of synaptic transmission and long-term potentiation: Effects on paired pulse facilitation and EPSC variance in the CA1 region of the hippocampus. *J Neurophysiol* 70(4):1451–1459.

53. Corlew R, Brasier DJ, Feldman DE, Philpot BD (2008) Presynaptic NMDA receptors: Newly appreciated roles in cortical synaptic function and plasticity. *Neuroscientist* 14(6):609–625.

54. Goriounova NA, Mansvelder HD (2012) Nicotine exposure during adolescence leads to short- and long-term changes in spike timing-dependent plasticity in rat prefrontal cortex. *J Neurosci* 32(31):10484–10493.

55. González-Maeso J, et al. (2003) Transcriptome fingerprints distinguish hallucinogenic and nonhallucinogenic 5-hydroxytryptamine 2A receptor agonist effects in mouse somatosensory cortex. *J Neurosci* 23(26):8836–8843.

56. Millan MJ, et al. (2012) Cognitive dysfunction in psychiatric disorders: Characteristics, causes and the quest for improved therapy. *Nat Rev Drug Discov* 11(2):141–168.

57. Sjöström PJ, Turrigiano GG, Nelson SB (2001) Rate, timing, and cooperativity jointly determine cortical synaptic plasticity. *Neuron* 32(6):1149–1164.

58. Kim J, et al. (2004) Sindbis vector SINrep(nsP2S726): A tool for rapid heterologous expression with attenuated cytotoxicity in neurons. *J Neurosci Methods* 133(1-2):81–90.

59. Toda S, Shen HW, Peters J, Cagle S, Kalivas PW (2006) Cocaine increases actin cycling: Effects in the reinstatement model of drug seeking. *J Neurosci* 26(5):1579–1587.

60. Phillips GR, et al. (2001) The presynaptic particle web: Ultrastructure, composition, dissolution, and reconstitution. *Neuron* 32(1):63–77.